



Cite this: *Phys. Chem. Chem. Phys.*,
2016, **18**, 33351

Phase engineering of MoS₂ through GaN/AlN substrate coupling and electron doping†

Bin Ouyang,^a Pengfei Ou,^a Yongjie Wang,^b Zetian Mi^b and Jun Song^{*a}

The polymorphism of two dimensional MoS₂ promises new possibilities for nanoelectronics. The realization of those possibilities necessitates techniques to enable flexible and controllable phase engineering of MoS₂. In the present study, based on first-principles calculations, a new and flexible route to engineer the phase stability of MoS₂ by interfacing it with a GaN or AlN substrate is reported. Depending on the surface termination of the underlying substrate, MoS₂ may exhibit either the 2H or 1T' (1T'') phase. The interface coupling between MoS₂ and the substrate also affects the phase transition kinetics. In addition, electron doping can act as another means to influence MoS₂-substrate interactions and enable further phase engineering of MoS₂. The present findings contribute to new knowledge towards phase engineering of MoS₂ and the design of hybrid nanodevices comprising both 2D and 3D optoelectronic materials.

Received 3rd August 2016,
Accepted 17th November 2016

DOI: 10.1039/c6cp05404h

www.rsc.org/pccp

1. Introduction

Among the wide variety of two dimensional materials and their related heterostructures discovered to date, monolayer MoS₂ has potential applications in optoelectronics,^{1–11} piezoelectronics^{12,13} and valleytronics.^{14–16} Regularly, exfoliated monolayer MoS₂ consists of an S–Mo–S sandwich structure with *P6̄m2* symmetry, which is called the 2H phase. As monolayer 2H-MoS₂ is a direct band gap semiconductor, it enables the design of two dimensional nanodevices, such as LED,^{2–4,6–8} solar cell,^{3,9–11} and nano power generator.¹³

Recently, the polymorphism of MoS₂ has attracted considerable attention.^{17–23} On one hand, the polymorphic phases enrich the electronic properties of monolayer MoS₂. More specifically, 1T-MoS₂ is metallic and can be used for hydrogen evolution and electrochemical devices like lithium/sodium batteries.^{24–28} The two distorted versions of the 1T phase, *i.e.* 1T' and 1T'' phase, are near metallic with a band gap smaller than 0.1 eV and have potential applications, such as in two dimensional topological insulators.^{15,29,30} On the other hand, different structural phases can be recombined, which would yield an inherent heterostructure with a coherent interface among 2H/1T (1T' or 1T'') phases. Owing to their compositional equality, the inherent heterostructures bring more flexibility in designing MoS₂-based nanotransistors^{20,31,32} or optoelectronic devices.^{33,34}

To better exploit the distinct properties of those phases, one needs to be able to control the phase transition within MoS₂. The state-of-the-art methods to enable phase transition in MoS₂ include lithium intercalation,^{17,18,21} defect (vacancy, doping) engineering,^{19,20,35} electrostatic gating,²² and strain engineering,²³ among others. However, lithium intercalation and defect engineering necessarily modify the defect structure and distribution within an MoS₂ sheet,^{19,21,36} thereby altering the properties of the resultant MoS₂ phases. On the other hand, the application of the electrostatic gating and strain engineering is limited by the electron density and/or elastic strain attainable in experiments.^{22,23,37} In view of the abovementioned limitations, new routes to achieve phase engineering are still needed.

In this study, utilizing density functional theory (DFT) calculations, we report a new way to engineer phase transitions in MoS₂ by interfacing it with a GaN or AlN substrate. With similar application in the field of optoelectronics, there have already been several experimental^{38,39} and theoretical^{40,41} studies in MoS₂/GaN (AlN) heterostructures. However, research discussing the interface interaction and phase stabilities of MoS₂ is still absent. Therefore, in this study, we focus on the interaction between MoS₂ and *c*-plane GaN or AlN. The role of surface termination of the *c*-plane surface on the phase stabilities of different MoS₂ phases and associated phase transition kinetics were studied. In addition, electron doping as a means to influence the MoS₂-substrate interactions and to enable further phase engineering of MoS₂ was examined. In the end, the implications of these results on phase engineering of MoS₂ and the design of devices comprising both 2D and 3D optoelectronic materials were discussed.

^a Department of Mining and Materials Engineering, McGill University, Montreal, QC, H3A 0C5, Canada. E-mail: jun.song2@mcgill.ca

^b Department of Electrical and Computer Engineering, McGill University, Montreal, QC, H3A 0E9, Canada

† Electronic supplementary information (ESI) available. See DOI: 10.1039/c6cp05404h

2. Computational methodology

First-principles DFT calculations employing the Perdew–Burke–Ernzerhof (PBE) functional⁴² and projector augmented-wave (PAW)⁴³ method were performed using the Vienna *ab initio* simulation package (VASP).⁴⁴ The simulation cell comprises a monolayer, MoS₂, sitting on top of a substrate consisting of six layers of a GaN or AlN slab with a [0001] facet, as illustrated in Fig. 1. Benchmark calculations were performed showing that the GaN and AlN slab models, considered, are energetically stable (see ESI†). The dispersive van der Waals interactions between the MoS₂ monolayer and underlying GaN (AlN) substrate were included using the DFT-D2 method of Grimme.^{45–47} A vertical vacuum space of a dimension >2 nm (along the direction perpendicular to the MoS₂ sheet) was used to eliminate the periodic image interactions. A 2 × 2 supercell of GaN (AlN) slab was paired with a 2 × 2 supercell of 2H-MoS₂, 1 × 2 supercell of 1T'-MoS₂ or 1 × 1 super cell of 1T''-MoS₂ to create the heterostructure model. It is important to note that those MoS₂ phases as well as the GaN and AlN substrates exhibit different lattice constants (see Table S1 in the ESI†). However, for simplicity, we assume a commensurate interface between MoS₂ and the underlying GaN (AlN) substrate, and that the lattices of all systems conform to that of 2H-MoS₂. A 7 × 7 × 1 *k*-point grid and cutoff energy of 500 eV were used in all calculations. It is worth mentioning that spontaneous polarization,⁴⁸ a phenomenon often present in GaN (AlN), was not considered in the present study.

One aspect worth discussing is the structure of the (0001) GaN and AlN surfaces. As reported in several studies, the (0001) surface can undergo surface reconstruction, particularly when influenced by the external chemical environment.^{49–52} For instance, Smith *et al.* reported Ga adatoms induced reconstruction of GaN(0001) surface,⁴⁹ and Li *et al.* reported the surface reconstruction of GaN(0001) triggered by the deposition of

Co atoms.⁵⁰ Nonetheless, unreconstructed (0001) surfaces can be achieved in experiments,^{53,54} when the surface is properly cleaned to remove contamination.^{55,56} In the present study, we assume the (0001) GaN and AlN surfaces to remain unreconstructed for simplicity. Benchmark studies have been conducted to demonstrate that the (0001) GaN and AlN surfaces are at least energetically metastable (see ESI†).

At the interface, MoS₂ may be in contact with either metal (Ga or Al) atoms or N atoms, depending on the Ga or N termination of the GaN (AlN) *c*-plane surface, *i.e.* (0001) or (000 $\bar{1}$) surface. This, along with the relative lateral shift of the MoS₂ sheet with respect to the GaN (AlN) substrate, leads to several possible interface configurations. To distinguish the different interface configurations, a notation of format P/T_{XY} was utilized, where P stands for the phase type of MoS₂ (being either 2H, 1T, 1T' or 1T''), T stands for the type of terminated atoms, being either M (Ga or Al) or N, and XY represents the stacking sequence of MoS₂ on the GaN (AlN) substrate. In particular, X and Y indicate the standing sites of Mo and the S atoms on the (0001) surface of GaN (AlN) respectively. As illustrated in Fig. 1a, there are three types of lattice sites on the (0001) surface of GaN (AlN), labeled sites A, B and C. Sites A and B denote the lattice locations occupied by the top and second layers of atoms in GaN (AlN), and site C refers to the center of the hexagon constituted by sites A and B. With the parameters, P, T, X and Y decided, the interface configuration is fully prescribed.

Phonon calculations were also performed to examine the phase stability of structures. Density Functional Perturbation Theory (DFPT) calculations were used to yield the real space force constant matrix $\tilde{C}_{1x,1\beta}(q)$

$$\tilde{C}_{1x,1\beta}(q) = -\frac{\partial^2 E}{\partial u_i^\alpha(q) \partial u_j^\beta(q)} \quad (1)$$

being the second derivative of energy E with respect to displacements $u_i^\alpha(q)$ and $u_j^\beta(q)$, where q is the wave vector and $u_i^\phi(q)$ ($\phi = \alpha, \beta, i = I, J$) indicates the displacement of atom i along direction ϕ . With the force constant matrix determined, the phonon frequencies $\omega(q)$ can be obtained by solving the secular equation below:

$$\left| \frac{1}{\sqrt{M_1 M_2}} \tilde{C}_{1x,1\beta}(q) - \omega^2(q) \right| = 0, \quad (2)$$

where M_1 and M_2 are the atomic masses of atoms I and J, respectively.

The criteria of convergence for calculations of vibrational properties are set as 10⁻⁸ eV for electronic relaxation and 10⁻⁵ eV Å⁻¹ for ionic relaxation. Higher precision settings than these convergence criteria were tested and negligible difference in calculation results were found. The PHONOPY⁵⁷ package is employed with q grid of 17 × 17 × 1 applied for all the structures considered.

3. Results and discussion

3.1. Energetics and stability of MoS₂ phases

Defining the energy of a configuration P/T_{XY}, $E(P/T_{XY})$, as

$$E(P/T_{XY}) = E_{\text{total}}(P/T_{XY})/N_{\text{MoS}_2} \quad (3)$$

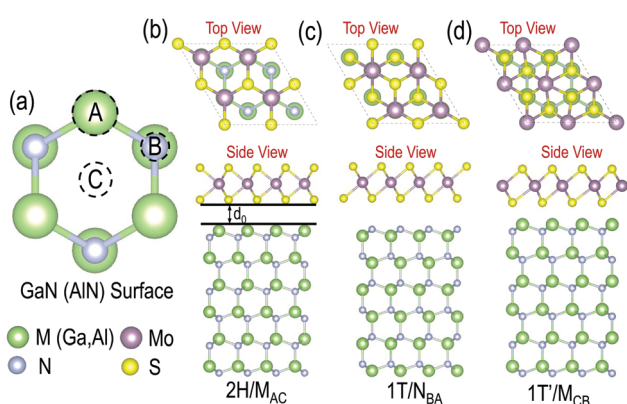


Fig. 1 (a) Top projection view of the *c*-plane surface of GaN or AlN, where A, B and C denotes the three possible standing sites for Mo and S. Three example stacking combinations are illustrated, being (b) 2H/M_{AC}, a 2H phase sitting on the (0001) surface of GaN (AlN) with Mo and S directly on top of sites A and C respectively, (c) 1T/N_{BA}, a 1T phase sitting on the (000 $\bar{1}$) surface of GaN (AlN) with Mo and S directly on top of sites B and A, respectively, and (d) 1T'/M_{CB}, a 1T' phase sitting on the (0001) surface of GaN (AlN) with Mo and S directly on top of sites C and B, respectively. Parameter d_0 refers to the equilibrium distance between the GaN (AlN) substrate and MoS₂.

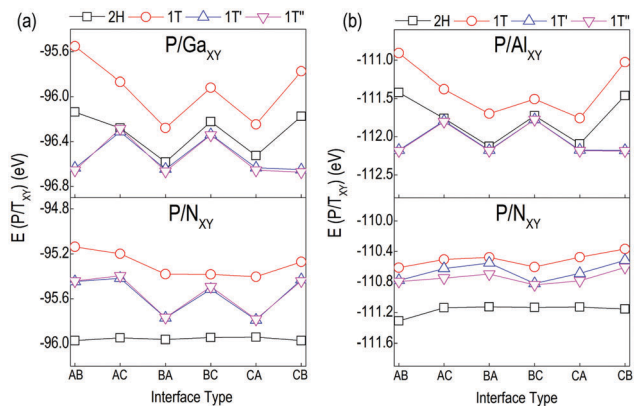


Fig. 2 Calculated total energy $E(P/T_{XY})$ of systems comprising of different MoS_2 phases on top of (a) Ga-terminated (top left) and N-terminated (bottom left) c -plane GaN, and (b) Al-terminated (top right) and N-terminated (bottom left) c -plane AlN.

where $E_{\text{total}}(P/T_{XY})$ represents the total energy of the system and N_{MoS_2} is the number of MoS_2 units in the simulation cell, we examined the energies of different MoS_2 -GaN and MoS_2 -AlN heterostructure configurations, and the results are shown in Fig. 2. For a MoS_2 monolayer sitting on top of the (0001) surface, its preferable phase is always either $1\text{T}'$ or $1\text{T}''$ regardless of the stacking XY, whereas the preferable phase becomes 2H when a MoS_2 monolayer interfaces with the (000 $\bar{1}$) surface. To better illustrate the energy difference between different configurations, all the calculated energy data are tabulated in the ESI.† It is also worth noting that the 1T phase always exhibits the highest energy. In addition, there is an apparent dependence of $E(P/T_{XY})$ on the stacking sequence XY.

The results, shown in Fig. 2, essentially show the relative stability of different MoS_2 phases on a GaN (AlN) substrate. The phase stability can be investigated further through phonon dispersion calculations, as illustrated in Fig. 3. Partial phonon density of states (PPDOS) associated with Mo and S atoms are extracted to elucidate the phase stability of MoS_2 for different interface configurations. Stacking sequences with the lowest energy are selected according to the calculation results presented in Fig. 2 so that AB stacking for GaN and AlN with metal or N termination are studied as a result. For each time of termination, PPDOS from four types of phases, *i.e.*, 2H, 1T, $1\text{T}'$ and $1\text{T}''$, are demonstrated on each subfigure (Fig. 3). Fig. 3 shows that for both metal terminations, imaginary frequencies are observed for 2H- MoS_2 s and 1T- MoS_2 s, while only positive frequencies can be observed for $1\text{T}'$ - MoS_2 s and $1\text{T}''$ - MoS_2 s. On the other hand, for N termination, only 2H- MoS_2 shows positive frequencies, while 1T, $1\text{T}'$, and $1\text{T}''$ phase possess imaginary branches of phonon frequency. These observations are consistent and further support the corresponding energetic results in Fig. 2, which show 2H- MoS_2 and 1T- MoS_2 having higher energies than $1\text{T}'$ - MoS_2 and $1\text{T}''$ - MoS_2 on a metal-terminated GaN (AlN) substrate. Therefore, it was confirmed that phase stability can be tailored by the surface polarity of GaN (AlN) substrates. It should be noted that in our calculations, the $1\text{T}'$ and $1\text{T}''$ phases were slightly strained as they were made to conform to the lattice of the 2H phase.

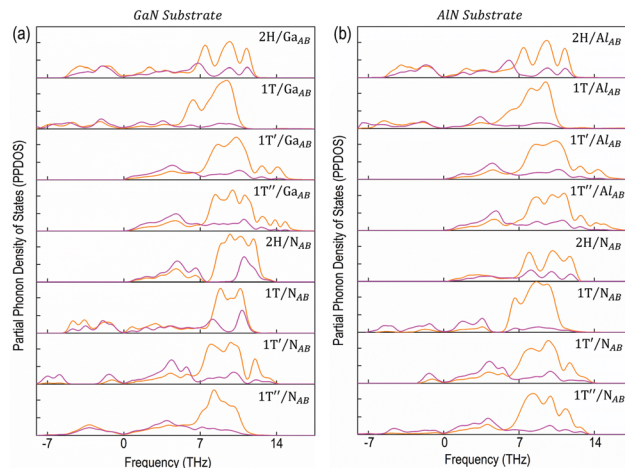


Fig. 3 Calculated partial Phonon Density of States (PPDOS) for MoS_2 phases on (a) Ga-terminated (top left) and N-terminated (bottom left) c -plane GaN substrates, and (b) Al-terminated (top right) and N-terminated (bottom right) c -plane AlN substrates.

Such straining can cause modification of the energetics, but it is not expected to change the overall picture of phase instability and transition in MoS_2 (see details in ESI†).

3.2. Role of interface on phase stability

The results shown above provide evidence that phase stability is influenced greatly by the MoS_2 -GaN (AlN) interface. To understand the physical origin underlying the interface effect, we examined the deformation charge density; representative cases are shown in Fig. 4. Note that the 1T phase of MoS_2 is always unstable (see Fig. 2 and prior discussion) and thus we have not included it in Fig. 4. For a substrate of metal termination, there is significant charge transfer between MoS_2 and the underlying substrate. This is expected because Ga and Al atoms have lower electronegativities than Mo and S and thus, tend to lose electrons. In addition, the level of charge transfer is considerably higher for $1\text{T}'$ and $1\text{T}''$ MoS_2 than for 2H MoS_2 , indicating that $1\text{T}'$ and $1\text{T}''$ MoS_2 form a much

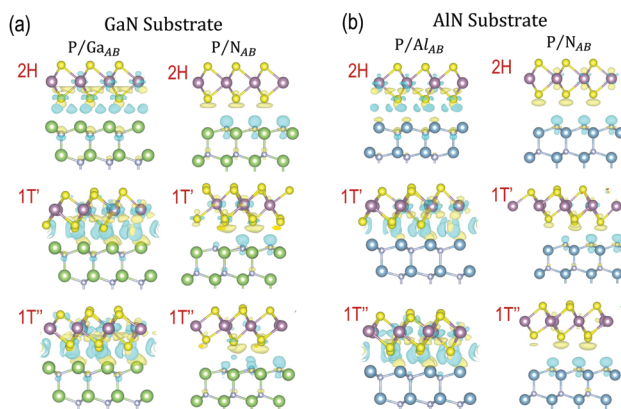


Fig. 4 Representative deformation charge density plots for MoS_2 phases on (a) Ga-terminated and N-terminated c -plane GaN substrates, and (b) Al-terminated and N-terminated c -plane AlN substrates.

Table 1 Values of \bar{E}_w , being the average of $E_w(P/T_{XY})$ over all stacking XY for different MoS₂–GaN (AlN) heterostructures. The notations, M_{XY} and N_{XY}, respectively, indicate whether the c-plane substrate is metal- or N-terminated, i.e., (0001) or (000 $\bar{1}$) surface

	\bar{E}_w (eV)					
	2H/M _{XY}	1T'/M _{XY}	1T''/M _{XY}	2H/N _{XY}	1T'/N _{XY}	1T''/N _{XY}
GaN	0.64 ± 0.22	1.38 ± 0.21	1.46 ± 0.20	0.18 ± 0.09	0.36 ± 0.11	0.37 ± 0.11
AlN	0.80 ± 0.35	1.67 ± 0.18	1.72 ± 0.21	0.15 ± 0.01	0.30 ± 0.06	0.29 ± 0.11

stronger binding with the (0001) surface, and thus are energetically favored (*cf.* Fig. 2).

On the other hand, for a substrate of N termination, there appears to be minimal charge transfer between MoS₂ and the substrate, suggesting weak mutual interactions. Therefore, one would expect that the substrate has little influence on the phase stability of MoS₂ and consequently 2H remains the most stable phase, which is consistent with the results in Fig. 2.

The abovementioned observations can be confirmed by examining the work of adhesion, E_w , at an interface configuration P/T_{XY},

$$E_w(P/T_{XY}) = [E(\text{MoS}_2^P) + E_S - E_{\text{total}}(P/T_{XY})]/N_{\text{MoS}_2}, \quad (4)$$

where $E(\text{MoS}_2^P)$ denotes the energy of a free-standing MoS₂ sheet of phase P and E_S denotes the energy of the substrate, while $E_{\text{total}}(P/T_{XY})$ is previously defined in eqn (3). The average value of $E_w(P/T_{XY})$ and over all stacking XY, namely \bar{E}_w , are listed in Table 1 (see ESI† of $E_w(P/T_{XY})$ for individual stacking).

As shown in Table 1, \bar{E}_w generally exhibits rather small values when the substrate is N-terminated, suggesting weak interaction between MoS₂ and the underlying substrate. On the other hand, when the substrate is metal-terminated, \bar{E}_w exhibits considerably higher values. In particular, the value of \bar{E}_w in the case of MoS₂ being 1T' or 1T'' is about two times as large as the one in the case of 2H MoS₂, which indicates that 1T' (1T'') MoS₂ has much stronger interaction with the substrate than 2H MoS₂.

3.3. Kinetics of phase transition

In addition to the energetics, another important aspect pertinent to phase stability of MoS₂ on the GaN (AlN) substrate is the kinetics. As previously noted, the energetically preferable phases are 1T' (1T'') and 2H for MoS₂ on metal- and N-terminated substrates, respectively. Therefore, we investigated the phase transitions between 2H and 1T' (1T''). For simplicity, we focus our discussion on MoS₂–GaN (AlN) heterostructures of the AB stacking as representatives. The minimum energy paths (MEPs) and corresponding transition-states (see Fig. S6 in the ESI†) associated with the phase transitions were examined, and the values of activation barriers are tabulated in Table 2. The activation barrier E_b ranged from 0.54 to 1.56 eV per u.c. First, one can note that E_b associated with 2H → 1T' (and 1T' → 2H) are similar to the one associated with 2H → 1T'' (and 1T'' → 2H). This is well expected given the similarity in energetics and charge transfer behaviors of 1T' and 1T'' on the GaN or AlN substrate (*cf.* Fig. 2–3). Second, the barriers associated with 2H → 1T' (1T'') transition are barely affected by the substrate, as evidenced by them being close to the ones of free-standing MoS₂. On the other hand, the barriers associated with 1T' (1T'') → 2H

Table 2 Activation barrier E_b (normalized by the number of MoS₂ units) for phase transitions between 2H and 1T' (1T''), for the representative stacking sequence AB

		E_b (eV per u.c.)			
		2H → 1T'	2H → 1T''	1T' → 2H	1T'' → 2H
GaN	P/Ga _{AB}	1.06	1.04	1.56	1.56
	P/N _{AB}	1.08	1.07	0.54	0.55
AlN	P/Al _{AB}	1.08	1.08	1.34	1.35
	P/N _{AB}	1.04	1.04	0.51	0.52
Free-standing MoS ₂		0.90	0.95	0.29	0.34

increase compared to the ones associated with free-standing MoS₂. The increase in the activation barrier is particularly significant when the substrate is metal-terminated, which can be attributed to the strong interaction between 1T' (1T'') MoS₂ and metal-terminated substrates, as previously discussed (*cf.* Fig. 4 and Table 1). In the kinetic terms, this increase in barrier would help stabilize the 1T' (1T'') phase on the GaN or AlN substrate.

3.4. Further tuning of phase stability via electron doping

As seen in Section 3.2., the influence of the substrate on phase instability of MoS₂ is mainly attributed to the charge transfer between MoS₂ and the substrate. In particular, for the cases of metal-terminated substrates, the substrate loses electrons or effectively “injects” electrons to MoS₂. Therefore, the substrate engineering of MoS₂ can naturally couple with charge injection. The ability of electron doping to further tune the phase stability of MoS₂ (on a metal-terminated GaN or AlN substrate) is discussed below.

For electron doping density ranging from $-0.5q_0$ to $0.5q_0$ ($q_0 = 1.6 \times 10^{-19}$ C per u.c.), it was found that electron doping can induce a phase transition for interface configurations P/M_{AC}, P/M_{BA}, P/M_{BC} and P/M_{CA} (M = Ga or Al) in MoS₂–GaN (AlN) heterostructures (rest of the situations can be found in the ESI†). The influence of electron doping can be evaluated as follows:

$$\Delta E^q(P/M_{XY}) = E^q(P/M_{XY}) - E^0(2H/M_{XY}), \quad (5)$$

where $E^q(P/M_{XY})$ denotes the energy of the configuration P/M_{XY} at an electron doping density of q , while $E^0(2H/M_{XY})$ denotes the energy of the corresponding 2H/M_{XY} without electron doping. Both $E^q(P/M_{XY})$ and $E^0(2H/M_{XY})$ are defined in a similar way as mentioned in eqn (3). As shown in Fig. 5, 1T' (1T'') remains the preferred phase when the system is doped by a negative charge, while the 1T' (1T'') → 2H transition can be triggered by the injection of a positive charge (except for the case of P/Ga_{XY}, where 1T' becomes the preferred phase again

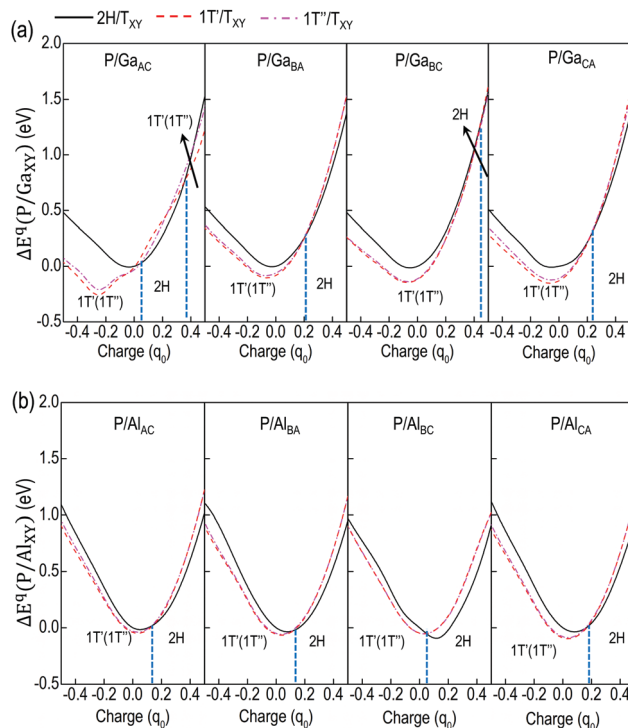


Fig. 5 Influence of electron doping on the energetics (*i.e.*, $\Delta E^q(P/M_{XY})$, see eqn (5)) of different MoS₂ phases on (a) Ga-terminated *c*-plane GaN substrates of interface configurations Ga_{AC}, Ga_{BA}, Ga_{BC}, and Ga_{CA}, and (b) Al-terminated *c*-plane AlN substrates of interface configurations Al_{AC}, Al_{BA}, Al_{BC}, and Al_{CA}.

Table 3 Threshold charge density for the 1T' (1T'') → 2H transition in GaN (AlN) supported MoS₂ sheet. The value of q is in the unit of q_0 , with $q_0 = 1.6 \times 10^{-19}$ C per u.c.

	Threshold doping density $q(q_0)$			
	P/M _{AC}	P/M _{BA}	P/M _{BC}	P/M _{CA}
GaN	0.05	0.20	0.43	0.21
AlN	0.14	0.12	0.05	0.17

under excessive doping of a positive charge, *i.e.*, $q > 0.36q_0$). The abovementioned effects of electron doping can be explained by in Fig. 4, where one can observe that the underlying metal-terminated GaN or AlN substrate loses its electrons to MoS₂. The injection of a positive charge effectively neutralizes those electrons, and thus weakens the interaction between MoS₂ and its underlying substrate, eventually resulting in a transition of 1T' (1T'') to the 2H phase for MoS₂. The values of electron doping density corresponding to the 1T' (1T'') → 2H transition are listed in Table 3. These values are all well within the range of density achievable through, *e.g.*, doping,^{35,36,58} electrostatic gating^{22,37} or external electric field,³⁷ in the experiments, suggesting that electron doping is a feasible route in device applications.

4. Conclusion

Utilizing density functional theory, phase stability and transition in MoS₂ interfacing with a *c*-plane GaN or AlN substrate

was studied. It was revealed that the relative phase stability and phase transition kinetics of MoS₂ can be manipulated by altering the surface termination of the underlying GaN or AlN substrate. In particular, for cases where MoS₂ interfaces with a metal-terminated substrate and MoS₂, significant charge transfer occurs at the interface, leading to strong MoS₂–substrate interactions that favor 1T' (1T'') phases over the 2H phase. Such MoS₂–substrate interactions also substantially increase the activation barrier of 1T' (1T'') → 2H transition, which further contributes to stabilizing the 1T' (1T'') phase on metal-terminated GaN or AlN substrate. The phase stability of GaN (or AlN)-supported MoS₂ can be modified by employing electron doping. With the injection of positive charges, the energetically preferable phase of MoS₂, on a metal-terminated GaN or AlN substrate, can revert to the 2H phase. The present findings suggest a new route of phase engineering in MoS₂, *via* interface coupling with a GaN or AlN substrate and electron doping, contributing new knowledge towards the design of novel devices integrating 2D and 3D optoelectronic materials.

Acknowledgements

We greatly thank the financial support from McConnell Memorial Fellowship in Engineering, McGill Engineering Doctorate Award, and NSERC Discovery grant (grant # RGPIN 418469-2012). The authors would also like to acknowledge Supercomputer Consortium Laval UQAM McGill and Eastern Quebec for providing computing power.

References

- J. Feng, X. Qian, C.-W. Huang and J. Li, *Nat. Photonics*, 2012, **6**, 866–872.
- A. Splendiani, L. Sun, Y. Zhang, T. Li, J. Kim, C.-Y. Chim, G. Galli and F. Wang, *Nano Lett.*, 2010, **10**, 1271–1275.
- O. Lopez-Sanchez, E. Alarcon Llado, V. Koman, A. Fontcuberta i Morral, A. Radenovic and A. Kis, *ACS Nano*, 2014, **8**, 3042–3048.
- M. Buscema, M. Barkelid, V. Zwiller, H. S. J. van der Zant, G. A. Steele and A. Castellanos-Gomez, *Nano Lett.*, 2013, **13**, 358–363.
- X. Hong, J. Kim, S.-F. Shi, Y. Zhang, C. Jin, Y. Sun, S. Tongay, J. Wu, Y. Zhang and F. Wang, *Nat. Nanotechnol.*, 2014, **9**, 682–686.
- K. Roy, M. Padmanabhan, S. Goswami, T. P. Sai, G. Ramalingam, S. Raghavan and A. Ghosh, *Nat. Nanotechnol.*, 2013, **8**, 826–830.
- S. Tongay, J. Suh, C. Ataca, W. Fan, A. Luce, J. S. Kang, J. Liu, C. Ko, R. Raghunathanan, J. Zhou, F. Ogletree, J. Li, J. C. Grossman and J. Wu, *Sci. Rep.*, 2013, **3**, 2657.
- R. S. Sundaram, M. Engel, A. Lombardo, R. Krupke, A. C. Ferrari, P. Avouris and M. Steiner, *Nano Lett.*, 2013, **13**, 1416–1421.
- C.-H. Lee, G.-H. Lee, A. M. van der Zande, W. Chen, Y. Li, M. Han, X. Cui, G. Arefe, C. Nuckolls, T. F. Heinz, J. Guo, J. Hone and P. Kim, *Nat. Nanotechnol.*, 2014, **9**, 676–681.
- M. Bernardi, M. Palummo and J. C. Grossman, *Nano Lett.*, 2013, **13**, 3664–3670.

- 11 M. Palummo, M. Bernardi and J. C. Grossman, *Nano Lett.*, 2015, **15**, 2794–2800.
- 12 H. Zhu, Y. Wang, J. Xiao, M. Liu, S. Xiong, Z. J. Wong, Z. Ye, Y. Ye, X. Yin and X. Zhang, *Nat. Nanotechnol.*, 2015, **10**, 151–155.
- 13 W. Wu, L. Wang, Y. Li, F. Zhang, L. Lin, S. Niu, D. Chenet, X. Zhang, Y. Hao, T. F. Heinz, J. Hone and Z. L. Wang, *Nature*, 2014, **514**, 470–474.
- 14 K. F. Mak, K. He, J. Shan and T. F. Heinz, *Nat. Nanotechnol.*, 2012, **7**, 494–498.
- 15 N. F. Q. Yuan, K. F. Mak and K. T. Law, *Phys. Rev. Lett.*, 2014, **113**, 097001.
- 16 K. F. Mak, K. He, C. Lee, G. H. Lee, J. Hone, T. F. Heinz and J. Shan, *Nat. Mater.*, 2013, **12**, 207–211.
- 17 A. P. Nayak, T. Pandey, D. Voiry, J. Liu, S. T. Moran, A. Sharma, C. Tan, C.-H. Chen, L.-J. Li, M. Chhowalla, J.-F. Lin, A. K. Singh and D. Akinwande, *Nano Lett.*, 2015, **15**, 346–353.
- 18 L. Wang, Z. Xu, W. Wang and X. Bai, *J. Am. Chem. Soc.*, 2014, **136**, 6693–6697.
- 19 L. Cai, J. He, Q. Liu, T. Yao, L. Chen, W. Yan, F. Hu, Y. Jiang, Y. Zhao, T. Hu, Z. Sun and S. Wei, *J. Am. Chem. Soc.*, 2015, **137**, 2622–2627.
- 20 Y.-C. Lin, D. O. Dumcenco, Y.-S. Huang and K. Suenaga, *Nat. Nanotechnol.*, 2014, **9**, 391–396.
- 21 Y. Guo, D. Sun, B. Ouyang, A. Raja, J. Song, T. F. Heinz and L. E. Brus, *Nano Lett.*, 2015, **15**, 5081–5088.
- 22 B. Ouyang, G. Lan, Y. Guo, Z. Mi and J. Song, *Appl. Phys. Lett.*, 2015, **107**, 191903.
- 23 K.-A. N. Duerloo, Y. Li and E. J. Reed, *Nat. Commun.*, 2014, **5**, 4214.
- 24 H. Wang, Z. Lu, S. Xu, D. Kong, J. J. Cha, G. Zheng, P.-C. Hsu, K. Yan, D. Bradshaw, F. B. Prinz and Y. Cui, *Proc. Natl. Acad. Sci. U. S. A.*, 2013, **110**, 19701–19706.
- 25 M. A. Lukowski, A. S. Daniel, F. Meng, A. Forticaux, L. Li and S. Jin, *J. Am. Chem. Soc.*, 2013, **135**, 10274–10277.
- 26 M. Mortazavi, C. Wang, J. Deng, V. B. Shenoy and N. V. Medhekar, *J. Power Sources*, 2014, **268**, 279–286.
- 27 M. Acerce, D. Voiry and M. Chhowalla, *Nat. Nanotechnol.*, 2015, **10**, 313–318.
- 28 S. Zhang, B. V. R. Chowdari, Z. Wen, J. Jin and J. Yang, *ACS Nano*, 2015, **9**, 12464–12472.
- 29 X. Qian, J. Liu, L. Fu and J. Li, *Science*, 2014, **346**, 1344–1347.
- 30 J. J. Cha, K. J. Koski and Y. Cui, *Phys. Status Solidi RRL*, 2013, **7**, 15–25.
- 31 R. Kappera, D. Voiry, S. E. Yalcin, B. Branch, G. Gupta, A. D. Mohite and M. Chhowalla, *Nat. Mater.*, 2014, **13**, 1128–1134.
- 32 D. Jena, K. Banerjee and G. H. Xing, *Nat. Mater.*, 2014, **13**, 1076–1078.
- 33 G. Eda, T. Fujita, H. Yamaguchi, D. Voiry, M. Chen and M. Chhowalla, *ACS Nano*, 2012, **6**, 7311–7317.
- 34 B. Ouyang, Z. Mi and J. Song, *J. Phys. Chem. C*, 2016, **120**, 8927–8935.
- 35 Y. Zhou and E. J. Reed, *J. Phys. Chem. C*, 2015, **119**, 21674–21680.
- 36 D. Nasr Esfahani, O. Leenaerts, H. Sahin, B. Partoens and F. M. Peeters, *J. Phys. Chem. C*, 2015, **119**, 10602–10609.
- 37 Y. Li, K.-A. N. Duerloo, K. Wauson and E. J. Reed, *Nat. Commun.*, 2016, **7**, 10671.
- 38 E. W. Lee, C. H. Lee, P. K. Paul, L. Ma, W. D. McCulloch, S. Krishnamoorthy, Y. Wu, A. R. Arehart and S. Rajan, *Appl. Phys. Lett.*, 2015, **107**, 103505.
- 39 Y. Zhu, N. Jain, D. K. Mohata, S. Datta, D. Lubyshev, J. M. Fastenau, A. K. Liu and M. K. Hudait, *J. Appl. Phys.*, 2013, **113**, 024319.
- 40 C. He, W. X. Zhang, T. Li, L. Zhao and X. G. Wang, *Phys. Chem. Chem. Phys.*, 2015, **17**, 23207–23213.
- 41 J. Liao, B. Sa, J. Zhou, R. Ahuja and Z. Sun, *J. Phys. Chem. C*, 2014, **118**, 17594–17599.
- 42 J. Perdew, K. Burke and M. Ernzerhof, *Phys. Rev. Lett.*, 1996, **77**, 3865–3868.
- 43 P. E. Blöchl, *Phys. Rev. B: Condens. Matter Mater. Phys.*, 1994, **50**, 17953–17979.
- 44 K. F. Mak, C. Lee, J. Hone, J. Shan and T. F. Heinz, *Phys. Rev. Lett.*, 2010, **105**, 136805.
- 45 S. Grimme, S. Ehrlich and L. Goerigk, *J. Comput. Chem.*, 2011, **32**, 1456–1465.
- 46 S. Grimme, *J. Comput. Chem.*, 2006, **27**, 1787–1799.
- 47 S. Grimme, J. Antony, S. Ehrlich and H. Krieg, *J. Chem. Phys.*, 2010, **132**, 154104.
- 48 M. Leszczynski, H. Teisseyre, T. Suski, I. Grzegory, M. Bockowski, J. Jun, S. Porowski, K. Pakula, J. M. Baranowski, C. T. Foxon and T. S. Cheng, *Appl. Phys. Lett.*, 1996, **69**, 73–75.
- 49 A. R. Smith, R. M. Feenstra, D. W. Greve, M. S. Shin, M. Skowronski, J. Neugebauer and J. E. Northrup, *J. Vac. Sci. Technol., B: Microelectron. Nanometer Struct.–Process., Meas., Phenom.*, 1998, **16**, 2242–2249.
- 50 H. D. Li, G. H. Zhong, H. Q. Lin and M. H. Xie, *Phys. Rev. B: Condens. Matter Mater. Phys.*, 2010, **81**, 233302.
- 51 A. R. Smith, R. M. Feenstra, D. W. Greve, M. S. Shin, M. Skowronski, J. Neugebauer and J. E. Northrup, *Surf. Sci.*, 1999, **423**, 70–84.
- 52 M. Himmerlich, L. Lymperakis, R. Gutt, P. Lorenz, J. Neugebauer and S. Krischok, *Phys. Rev. B: Condens. Matter Mater. Phys.*, 2013, **88**, 125304.
- 53 V. Ramachandran, C. D. Lee, R. M. Feenstra, A. R. Smith, J. E. Northrup and D. W. Greve, *J. Cryst. Growth*, 2000, **209**, 355–363.
- 54 O. E. Tereshchenko, G. E. Shaibler, A. S. Yaroshevich, S. V. Shevelev, A. S. Terekhov, V. V. Lundin, E. E. Zavarin and A. I. Besyul'kin, *Phys. Solid State*, 2004, **46**, 1949–1953.
- 55 S. W. King, J. P. Barnak, M. D. Bremser, K. M. Tracy, C. Ronning, R. F. Davis and R. J. Nemanich, *J. Appl. Phys.*, 1998, **84**, 5248–5260.
- 56 M. Diale, F. D. Auret, N. G. van der Berg, R. Q. Odendaal and W. D. Roos, *Appl. Surf. Sci.*, 2005, **246**, 279–289.
- 57 A. Togo, F. Oba and I. Tanaka, *Phys. Rev. B: Condens. Matter Mater. Phys.*, 2008, **78**, 134106.
- 58 M. Kan, J. Y. Wang, X. W. Li, S. H. Zhang, Y. W. Li, Y. Kawazoe, Q. Sun and P. Jena, *J. Phys. Chem. C*, 2014, **118**, 1515–1522.